DGKN-A94

Neuroimaging Meets Machine Learning: Identifying Neuroimaging-derived Predictors of Hand Grip Strength Independent of Age, Sex, and Body Composition

Vera Komeyer[1 2 3], Simon Eickhoff[1 4], Jan Kasper[1 4], Christian Grefkes-Hermann[5 6 7], Kaustubh Patil[1 4], Federico Raimondo[1 4]

[1]Heinrich Heine University Düsseldorf, Institute of Systems Neuroscience, Düsseldorf, Deutschland; *[2]Research Centre Jülich, Institute for Neuroscience and Medicine - 7, Jülich, Deutschland*; *[3]Heinrich-Heine-University Düsseldorf, Department of Biology, Faculty of Mathematics and Natural Sciences, Düsseldorf, Deutschland*; *[4]Research Centre Jülich, Institute of Neuroscience and Medicine (INM-7: Brain and Behaviour), Jülich, Deutschland*; *[5]Goethe University Frankfurt and University Hospital Frankfurt, Department of Neurology, Frankfurt (Main), Deutschland*; *[6]University Hospital Cologne and Medical Faculty, University of Cologne, Department of Neurology, Köln, Deutschland*; *[7]Research Centre Juelich, Institute of Neuroscience and Medicine, Cognitive Neuroscience (INM-3), Jülich, Deutschland*

Background: Hand grip strength (HGS) is a cost-efficient and reliable measure in clinical practice and is even recognized by the WHO as key marker for vitality in aging populations [1]. While HGS reflects overall strength of a person, it is also closely related to physical disability, cognitive decline and mortality [2,8,5]. Despite its significance, the neural mechanisms governing HGS remain unclear. Our study systematically developed and evaluated the combination of neuroimaging-derived features with machine learning models to predict HGS. The aim was to identify models that are solely driven by brain information free from confounding factors such as sex, age and body composition to gain insights in the neural underpinnings of HGS.

Objectives: see Background.

Question: see Background.

Methods: We leveraged large-scale data from the UK Biobank [3] (N=22554-33136) to predict HGS from 9 neuroimaging-derived feature categories: Gray matter volume (GMV) [10], fALFF, LCOR, GCOR [7] (each 1088 ROIs), cortical thickness, white surface area, white matter hyperintensity (WMH) with PSMD [4], gray white contrast and a collection of 6 white matter microstructural characteristics (Fractional Anisotropy (FA), Mean Diffusivity (MD), free water volume fraction (ISOVF), orientation dispersion index (OD), intra-cellular volume fraction (ICVF), diffusion tensor mode (MO)). We used 80% of the data to independently train 7 algorithms for each of the 9 categories in a 5-fold (nested) cross validation (CV) (Fig. 1A). Features were univariately, linearly adjusted for six confounder setups (Fig. 1B). A final model was trained on the entire training data to predict HGS in 20% unseen subjects. The same analyses were performed on sex-split data to rule out non-linear sex influences on predictions. For the six most successful confound-free models we employed explainable AI methods (SHAP [6]) to determine the neuroimaging information predictive of HGS.

Results: The sex-mixed sample analysis identified GMV, white surface, fALFF and white matter as most predictive features (Fig. 1B). Predictability decreased noticeably when adjusting for sex and age, but didn't drop further when removing more confounders (Fig. 1B). Non-linear algorithms performed better than linear ones in the sex-age-adjusted scenario (Fig. 1B purple vs. blue). Non-linear approaches also showed superior performance in "sex-split" models, even after controlling for age (Fig. 1D). GMV, fALFF and white matter were most resilient for the very stringent confounder control (Fig. 1D). For these three feature categories XGBoost excelled other non-linear algorithms, leading to the six (3 per sex) best models: $r(m)_{GMV}$ = 0.18, $r(f)_{GMV}$ = 0.20; $r(m)_{fALFF}$ = 0.18, $r(f)_{fALFF}$ = 0.23; $r(m)_{WM}$ = 0.21, $r(f)_{WM}$ = 0.23 (Fig. 1F). Interpretative SHAP analyses reveiled GMV's importance in anterior globus pallidus (Fig. 2A, B) and microstructural characteristics of sensory input bundles to the thalamus and thalamo-cortical tracts (Fig. 2E, F) as neural correlates for successful, confound-free HGS predictions.

Conclusions: Our exhaustive evaluation of ML models and features from diverse MRI modalities identified six effective models for predicting HGS under stringent confounding constraints. Our results are in line with insights from functional neuroanatomy and bridge a gap between the micro- and macrolevel neuroscientific understanding of HGS as a vitality marker.

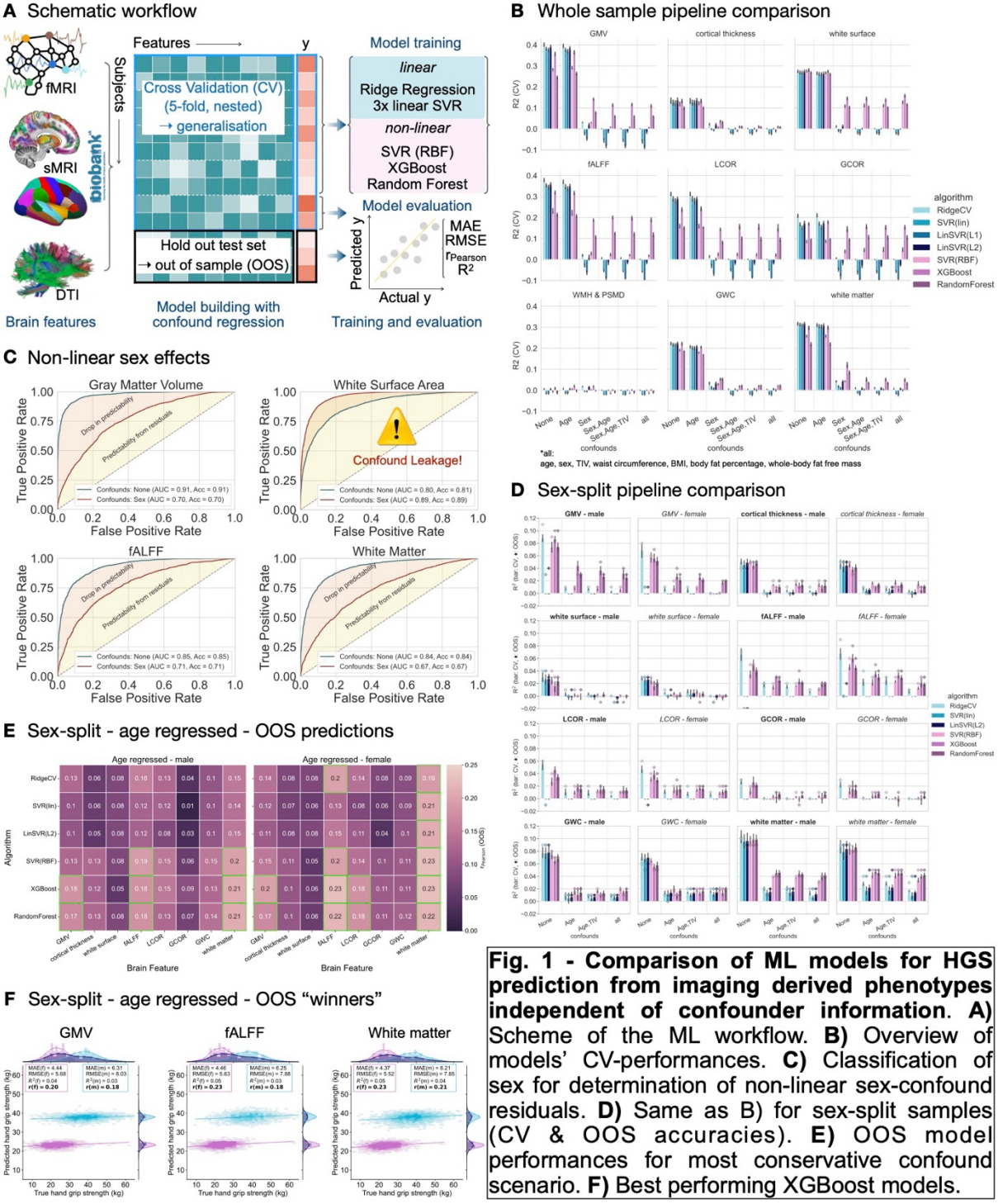

Fig. 1 - Comparison of ML models for HGS prediction from imaging derived phenotypes independent of confounder information. A) Scheme of the ML workflow. **B)** Overview of models' CV-performances. **C)** Classification of sex for determination of non-linear sex-confound residuals. **D)** Same as B) for sex-split samples (CV & OOS accuracies). **E)** OOS model performances for most conservative confound scenario. **F)** Best performing XGBoost models.

Abb. 1

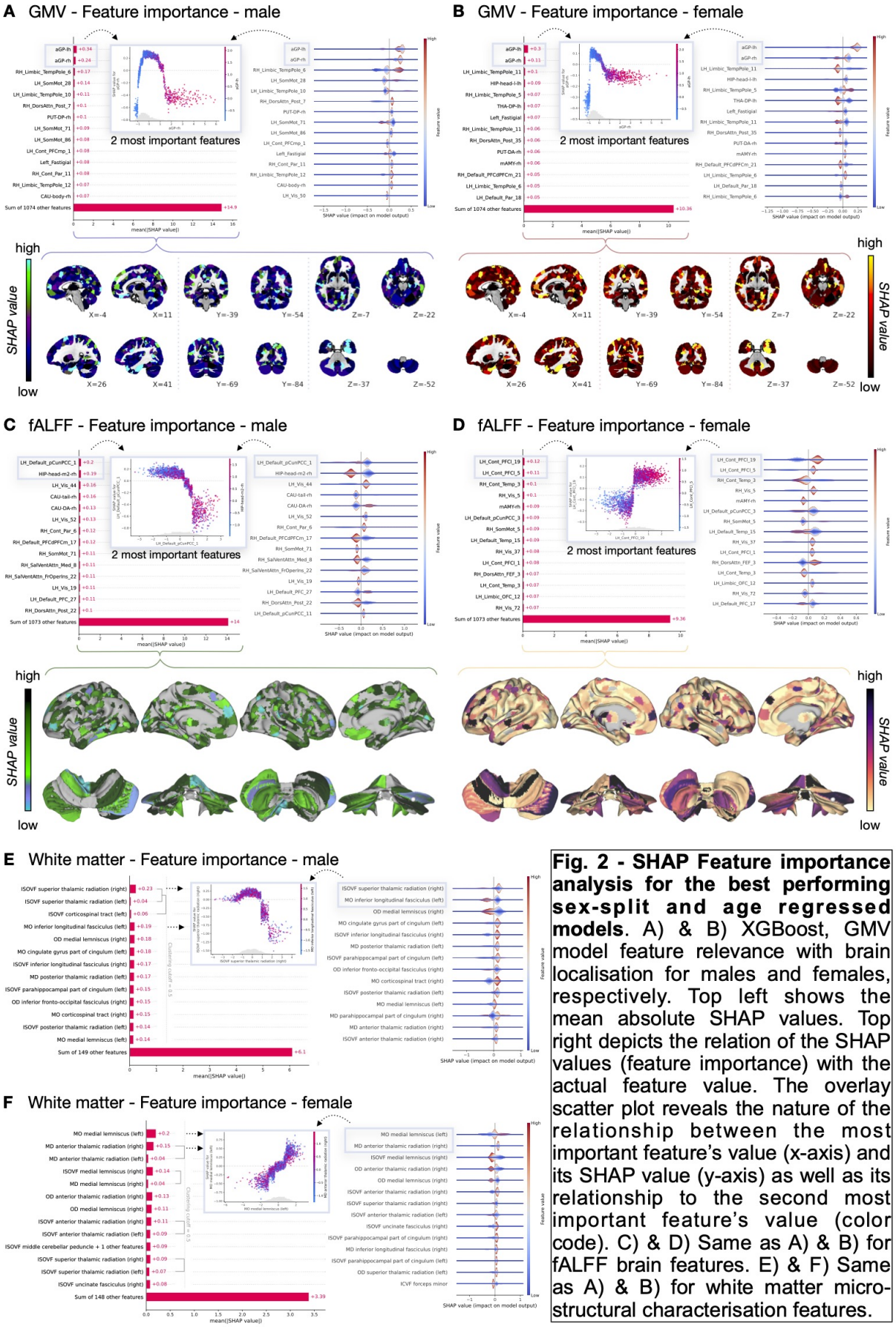

Fig. 2 - SHAP Feature importance analysis for the best performing sex-split and age regressed models. A) & B) XGBoost, GMV model feature relevance with brain localisation for males and females, respectively. Top left shows the mean absolute SHAP values. Top right depicts the relation of the SHAP values (feature importance) with the actual feature value. The overlay scatter plot reveals the nature of the relationship between the most important feature's value (x-axis) and its SHAP value (y-axis) as well as its relationship to the second most important feature's value (color code). C) & D) Same as A) & B) for fALFF brain features. E) & F) Same as A) & B) for white matter micro-structural characterisation features.

Abb. 2